SYNTHESIS, CHARACTERIZATION, AND GAS TRANSPORT PROPERTIES OF NEW COPOLY(ETHER-AMIDE)S CONTAINING BENZOPHENONE AROMATIC ISOPHTHALIC SEGMENT

JOSÉ LUIS SANTIAGO-GARCÍA[1], MARÍA ISABEL LORÍA-BASTARRACHEA[1], JULIO SÁNCHEZ[2], AND MANUEL AGUILAR-VEGA[1]*

[1]Grupo de Membranas, Unidad de Materiales. Centro de Investigación Científica de Yucatán A.C., Calle 43 No. 130, Col. Chuburná de Hidalgo, C.P. 97205, Mérida, Yuc., México.
[2]Departamento de Ciencias del Ambiente, Facultad de Química y Biología, Universidad de Santiago de Chile, USACH, Casilla 40, Correo 33, Santiago, Chile.

We congratulate the Chilean Chemical Society on its seventieth anniversary, and recognize all the members of the society who have helped to create the framework upon which the Society has grown and flourished.

ABSTRACT

Three new copoly(ether-amide)s based on polyether segments of different molecular weight (average molecular weight 400, 900 and 2000 g/mol) and polyamide segments obtained from 4,4'-diamine benzophenone (DBF) and isophthalic acid (ISO) are reported. The resulting new copoly(ether-amide)s have inherent viscosities ranging of 0.32 to 0.35 dL/g at concentration of 0.5 g/dL, and form dense membranes by solvent casting method. The gas transport properties of the new copoly(ether-amide) membranes for pure gases (He, CO_2, O_2, CH_4, and N_2) are studied at different pressures (2.0, 5.0, 7.5, and 10.0 atm) and at different temperatures (35-75 °C). The soft segment of polyether allows an increase in gas permeability coefficients, mainly CO_2, in comparison with the values reported for DBFISO aromatic polyamide. However, an increase in polyether segment length decreases the overall permeability coefficients, because the polyether shows a strong tendency to crystallize.

Keywords: copoly(ether-amide)s, membranes, permeability coefficients, gas separations.

1. INTRODUCTION

The development of new polymeric membranes with preferential CO_2 transport is hitherto an important research area, due to its high economic and environmental relevance[1]. CO_2 separation membrane technology in the energetic field can be used to switch to natural gas as a fuel and contribute to the reduction of carbon dioxide emissions[2,3]. Moreover, membrane technology has shown promising features due to its processability, relative ease of operation and control, it is also compact and easy to scale up as compared with conventional processes[4]. Presently, the traditional technologies to remove CO_2 from natural gas are mainly based on chemical and physical interactions; therefore the ability to capture CO_2 molecules is directly proportional to the affinity between CO_2 molecules and absorbent compounds[5,6,7]. The structural design of polymeric membranes has been shifting towards the fact of incorporating absorbent compounds, i.e. oxyethylene units, in the main chain polymer[8-13]. Block copolymer membranes have been explored recently as an alternative to reach this aim due to the fact that block segments with different gas transport properties can be combined[14].

In this respect, ethylene-oxide based copolymers, which present favorable interactions with CO_2, may be of interest to improve separation performance for CO_2 from natural gas[15,16,17]. Therefore, a strategy to design new membranes is the incorporation of polyether segments as soft blocks, due to the fact that pure polyether have a strong tendency to crystallize. Several researchers have developed membrane materials using this premise. This approach could not only form membranes that favor CO_2 transport but also achieve efficient solubility in polymers with rigid backbones[18].

In order to evaluate others polymeric systems, we have chosen to prepare block copolymers containing segments of aromatic polyamides, a very rigid material, which have high glass transition temperature and good mechanical strength. This aramide, poly(benzophenone)isophthalamide, DBFISO, that has been classified as an efficient gas barrier material, due to their high packing density, with low gas permeability coefficients reported such as 6.9×10^{-2} Barrer for O_2 and 3.3×10^{-1} Barrer for CO_2[19]. These barrier properties can be modified to design membranes that present gas permeability and selectivity to a specific gas, in this case CO_2, through the incorporation of segments with higher affinity to such gas molecule.

Here, we present the synthesis of new copoly(ether-amide) membranes that present improved gas transport properties as compared to those observed in pristine DBFISO aromatic polyamide. The new copoly(ether-amide)s were synthesized by condensation using the one pot-two step method, for the soft segment a commercial end amine terminated polyether (Jeffamine®) with three different molecular weights (400, 900 y 2000 g/mol) was combined with a hard segment based on a block from poly(benzophenone) isophthalamide obtained from 4,4'-diamine benzophenone (DBF) and isophthalic acid (ISO). The physical and chemical characteristics of the resultant block copoly(ether-amide)s were determined. Furthermore, the pure gas transport properties of the block copoly(ether-amide)s were determined at different pressures (2.0, 5.0, 7.5, and 10.0 atm) and temperatures (35-75 °C). This was done with the aim of correlating the effect of polyether segment size with gas transport properties of these materials.

2. EXPERIMENTAL SECTION

2.1. Materials and reagents

Isophthalic acid (ISO) and 4,4'-diaminobenzophenone (DBF) were purchased from Sigma-Aldrich Co., both monomers were used without further purification. *O*,*O*'-bis(2-aminopropyl)polypropylene glycol 300 (Jeffamine® D-400), *O*,*O*'-bis(2-aminopropyl)polypropylene glycol-block-polyethylene glycol-block-polypropylene glycol 800 (Jeffamine® ED-900) and *O*,*O*'-bis(2-aminopropyl)polypropylene glycol-block-polyethylene glycol-block-polypropylene glycol 1900 (Jeffamine® ED-2001) were purchased from Fluka and were dried in a desiccator at room temperature under vacuum for two days. Anhydrous *N*-methyl-2-pyrrolidone (NMP), dimethyl acetamide (DMAc), and deuterated dimethyl formamide (DMF-d_7) were purchased from Sigma-Aldrich Co. Triphenyl phosphite (TPP) and pyridine (Py) were stored over 4Å molecular sieves. Anhydrous calcium chloride ($CaCl_2$) and lithium chloride (LiCl) were dried under vacuum at 160 °C during 24 hours before being used.

2.2. Characterization techniques

FTIR spectra were recorded on a Nicolet Protégé 460 FTIR spectrometer at 4 cm^{-1} resolution and 100 scans in the absorption mode between 4000-400 cm^{-1}, using KBr discs with 2 % (w/w) of copolymer. The spectra were corrected for KBr background using the OMNIC software.

^{1}H-NMR spectra were recorded on a Bruker Avance 400 spectrometer in dueterated dimethylformamide (DMF-d_7) with 4.5 % (w/v) LiCl. Tetramethylsylane (TMS) was used as internal standard.

Differential scanning calorimetry (DSC) was performed in a differential scanning calorimeter DSC-7 Perkin-Elmer. Experiments were performed on 7.5 mg samples at a heating rate of 10 °C/min over the temperature range of -45 to 120 °C under nitrogen atmosphere.

The dynamic mechanical analysis (DMA) of the dense membranes was obtained using a DMA-7 analyzer (Perkin Elmer, Inc.). The sample specimens ($2.0\times15.0\times0.15$ mm) were analyzed in the tension mode at a constant frequency

e-mail: jlsantia@cicy.mx

of 1 Hz, and a temperature ranging from -100 to 200 °C, with a heating rate of 10 °C/min. The temperature corresponding to the peak in the loss tangent (tan δ) versus temperature plot was taken as the α-transition, which is closely related to the chain relaxations that give place to glass-transition temperature (T_g).

Thermogravimetric analysis was performed on a Thermobalance TGA-7 (Perkin Elmer, Inc.) under nitrogen atmosphere in the temperature range between 50 and 600 ºC at a heating rate of 10 ºC/min.

Inherent viscosities for all polymers were measured using an Ubbelohde viscosimeter, No. 50, with a polymer concentration of 0.5 g/dL in DMAc at 30 ± 0.1°C.

2.3. Copolymer synthesis

Three copoly(ether-amide)s were synthesized by direct polycondensation using triphenyl phosphite and pyridine as condensing agents to form amide bonds[20]. All copolymers were synthesized by a two-step one-pot approach as shown in Scheme 1. In the firt step, the reaction between diaminobenzophenone, DBF, and isophthalic acid, ISO, produced a hard segment as pre-polymer with carboxylic acid end groups, which were reacted later with one of the Jeffamines (400, 900 and 2000 g/mol) in the proper stoichiometric amounts to produce DI400, DI900 and DI2000 copoly(ether-amide)s. A typical example, using this reaction method for the segmented copoly(ether-amide)s synthesis was as follows: For the synthesis of the copoly(ether-amide) containing soft segments of Jeffamine® ED-2001 and a hard segment of DBFISO of 10 repeating units, average molecular weight ~3420, DI2000. A mixture of 2.75 mmol of ISO, 2.5 mmol of DBF, 0.562 g of $CaCl_2$ and 0.188 g of LiCl in 1.94 mL (7.42 mmol) of TPP, 1.92 mL (23.46 mmol) of Py, and 7.5 mL of NMP was heated with stirring at 105±2 °C for 2.5 h under a nitrogen atmosphere. To the reaction solution 0.25 mmol (0.5 g) of Jeffamine® ED-2001 was added, and the mixture was stirred for another 18 h at the same temperature. The copolymer was isolated by pouring the reaction mixture into 1 L of methanol with constant stirring. The product was a fibrous precipitated which was washed with methanol and hot water, collected on a filter, and dried under vacuum at less than 100 °C until constant weight. The other copoly(ether-amide)s were synthesized following the same procedure with the proper amounts of each Jeffamine®.

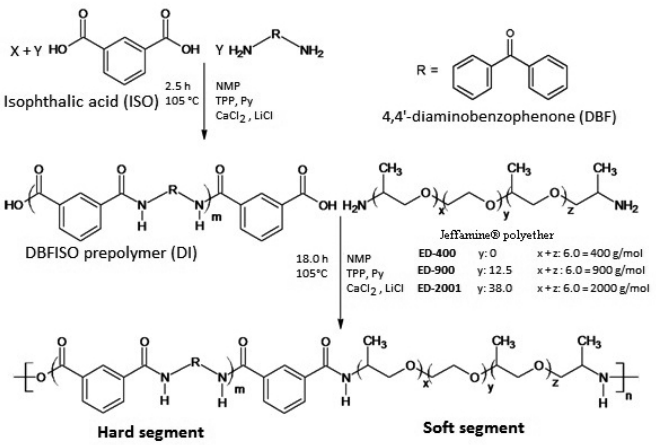

Scheme 1. Reaction scheme showing the synthesis of copoly(ether-amide) s by polycondensation using the one pot-two step method.

2.4. Preparation of dense membranes

Dense membranes were formed by casting using a solution containing 15 % (w/v) of polymer in dimethylacetamide (DMAc). The polymer solution was then filtered through a PTFE filter (0.45 µm) to remove dust particles and cast onto an aluminum ring mounted on a foil. The casting ring was covered with a glass bell with inlet and outlet of nitrogen gas. The solvent was eliminated by evaporation at 60 °C during 24 h under nitrogen atmosphere. Once the dense membrane was strong enough, it was removed from the foil and it was dried at 100 °C in a vacuum oven for two days to remove residual solvent. After the drying procedure, the thickness of membrane was measured with a Mitutoyo digital micrometer with a resolution of 1.0 µm.

2.5. Measurements of gas transport properties

Gas permeability coefficients for five different pure gases, He, O_2, CH_4, N_2, and CO_2, were measured in the same sequence using a permeation cell with the constant-volume method, which has been described elsewhere[21]. The surface area of the sample available for gas transport was 1.157 cm^2. Before carrying out any gas permeation experiment, the membranes were degassed during 24 h. Values of the transport coefficients of the pure gases through the membranes were determined at 35 °C for feed pressures of 2.0, 5.0, 7.5 and 10.0 atm. CO_2 permeability coefficients were also determined at a feed pressure of 2.0 atm at different temperatures between 35 and 75 °C in steps of 10 °C. The permeability coefficient, P, was determined from the slope of downstream pressure as a function of time after reaching steady state, and it is expressed in Barrer [1 Barrer = 1×10^{-10} $cm^3(STP)\,cm\,cm^{-2}\,s^{-1}\,cmHg^{-1}$]. Gas permeability coefficient, P, according to the solution-diffusion model is known to be the product of a diffusion coefficient, D, and a solubility coefficient, S.

$$P=D.S \qquad (1)$$

When a gas pressure is applied to one of the membrane faces, before reaching the steady state, the flux and the concentration vary with time at every point inside the membrane. The time necessary to reach steady state was used to determine the apparent diffusion coefficient, D, by the time lag (θ) approach by means of the equation:

$$D = \frac{l^2}{6\theta} \qquad (2)$$

where l is the membrane thickness. From these experimental values, the apparent solubility coefficient is then calculated as the ratio of P over D. The ideal selectivity of a membrane for gas A over gas B was determined as the ratio of their pure gas permeability coefficients:

$$\alpha_{A/B} = \frac{P_A}{P_B} \qquad (3)$$

3. RESULTS AND DISCUSSION

3.1. Synthesis and characterization of copoly(ether-amide)s

New copoly(ether-amide)s based on hard segments of diaminobenzophenone (DBFISO) and soft segments of polyether with different molecular weights were readily prepared in high yield (>92 %), according to the synthetic route depicted in Scheme 1. The copolymerization reaction was corroborated by FT-IR and ^{1}H-NMR spectroscopy. Figure 1 shows the stacked IR spectra of DBFISO aromatic prepolymer, Jeffamine® ED-2001, and copoly(ether-amide)s. The spectrum of DBFISO prepolymer shows the absorption bands due to N-H stretching at 3300 cm^{-1}, and C=O stretch at 1650 cm^{-1} (amide I) characteristic of aromatic polyamides (see Figure 1A). Whereas, the IR spectra of copoly(ether-amide)s show typical bands of DBFISO polyamides, together with those corresponding to the incorporated polyether segments at 1100 cm^{-1} (C-O-C) and 2880 cm^{-1} (C-H), indicating that both polyether segments and DBFISO aromatic prepolymer have reacted to form the copolymer (see Figure 1B).

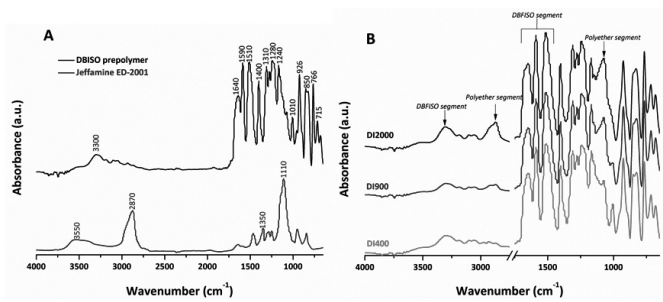

Figure 1. FTIR spectra from: A) DBISO prepolymer as hard segment and Jeffamine ED-2001 as soft polyether segment; B) DI2000, DI900, and DI400 copoly(ether-amide)s.

Figure 2 shows the stacked ^{1}H-NMR spectra of DBFISO aromatic prepolymer, Jeffamine® ED-2001, and block copoly(ether-amide)s. The amine-terminated polyether (Jeffamine® ED-2001) showed ^{1}H signal corresponding to methylenes (3.58 ppm), methyl group (1.10 ppm) and amino end groups (0.97 and 0.95 ppm) attached to the end of polyether backbone. The DBFISO

aromatic prepolymer showed a singlet signal attributed to the amide proton (10.92 ppm) and a multiplet at 7.70 and 8.50 ppm that belongs to aromatic C-H. The disappearance of the doublet at 0.97 and 0.95 ppm observed in the ^{1}H-NMR spectrum of the polyether and the presence of the singlet at 3.58 ppm and 1.10 ppm observed in the spectra of the block copoly(ether-amide)s confirmed that block copolymers were successfully synthesized by the method used here.

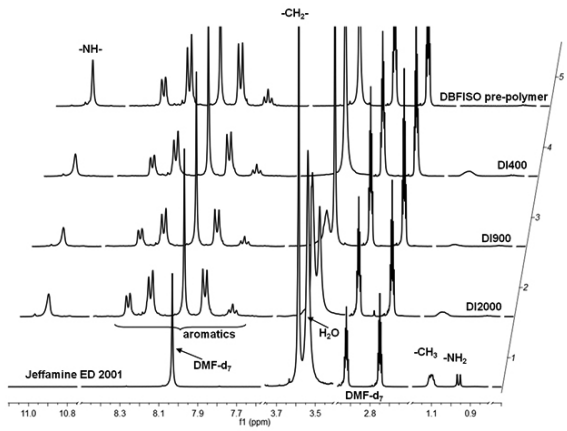

Figure 2. ^{1}H-NMR spectra of copoly(ether-amide)s synthesized and their component segments.

Table 1. Physical properties and molar composition of the copoly(ether-amide)s synthesized.

Copoly(ether-amide)s	ISO (mmol)	DBF (mmol)	Jeffamine® (mmol)	Yield (%)	Tg[d] (°C)	Tm (°C)	Char Yield 600°C	η_{inh} (dL/g)
DI400	2.75	2.5	0.25[a]	92.8	134	65	68.7	0.32
DI900	2.75	2.5	0.25[b]	93.5	120	66	65.5	0.35
DI2000	2.75	2.5	0.25[c]	92.6	83	69	59.6	0.34

[a]Jeffamine ED-400, *O,O*'-bis(2-aminopropyl)polypropylene glycol 300; [b](Jeffamine ED-900, *O,O*'-bis(2-aminopropyl)polypropylene glycol-block-polyethylene glycol-block-polypropylene glycol 800; [c]Jeffamine ED-2001, *O,O*'-bis(2-aminopropyl)polypropylene glycol-block-polyethylene glycol-block-polypropylene glycol 1900; [d]Determined by DMA.

Some physical properties of the copoly(ether-amide)s and their component segments are summarized in Table 1. The incorporation of soft polyether segments into a DBFISO aromatic polyamide affects the glass transition temperature. Since DSC measurements did not give a discernible glass transition temperature, T_g, for the polyether block of the copoly(ether-amide)s, it was attempted to determined its transition by DMA. The α-transition, which is the result of the same molecular process that give rise to T_g , found is -25 °C for the polyether block[22] and it is more discernible in DI2000 which has the largest polyether precursor of the copolyamides. The amide hard segment T_α appears at lower temperature due to the random introduction of polyether segments into the main chain by the one prepolymer method used[23]. Moreover, in the DSC analysis one characteristic melting temperature, T_m, was present in each sample (see Figure 3). The peak of the melting endotherm appeared at a slightly higher temperature as the molecular weight and ethylene oxide unit content increases in the soft segment, moving from 65 °C for DI400, to 66 °C for DI900, and to 69 °C for DI2000, which is consistent with those values reported by Lin and Freeman[15]. In addition, the melting enthalpy, obtained from the area under the melting endotherm, showed an increases (DI400=1.19 J/g, DI900=3.24J/g, DI2000=13.07 J/g) with increasing molecular weight of the polyether segment precursor Jeffamine. These results suggest that crystallinity (DI900, 0.71 %, DI900, 1.95 %, and DI2000, 7.85 %)[15] increases with increasing molecular weight of the soft segment a behavior that has been reported before[18].

The thermal stability of the block copoly(ether-amide)s was evaluated by TGA, and the decomposition thermograms are shown in Figure 4. The weight loss is different for each block copolymer with respect to their component segments, while that of the DBFISO prepolymer presents higher thermal stability due to the aromatic structure, with a weight loss at 500 °C of 17 wt % (w/w), the aliphatic Jeffamine® ED-2001 decomposes completely at 450 °C. Therefore, the block copoly(ether-amide)s present lower thermal stability than the DBFISO homopolyamides adscribed to the lower stability of the ether link (C-O) in the polyether chain. This fact allowed to estimate the polyether content in the copoly(ether-amide)s synthesized. The result indicates that DI400= 5.34 %, DI900= 8.49 %, and DI2000= 14.46 % that almost triplicates the polyether content in the block copolyether-amide prepared from DI400 to the one prepared from DI2000.

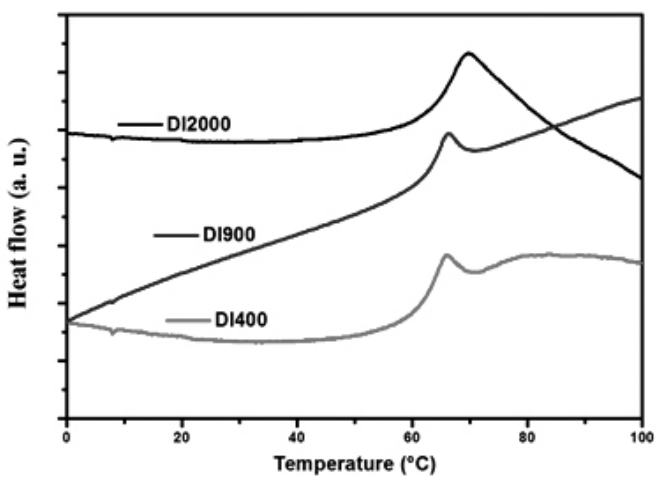

Figure 3. DSC thermograms of copoly(ether-amide)s. First scan at 10 °C/min under nitrogen atmosphere

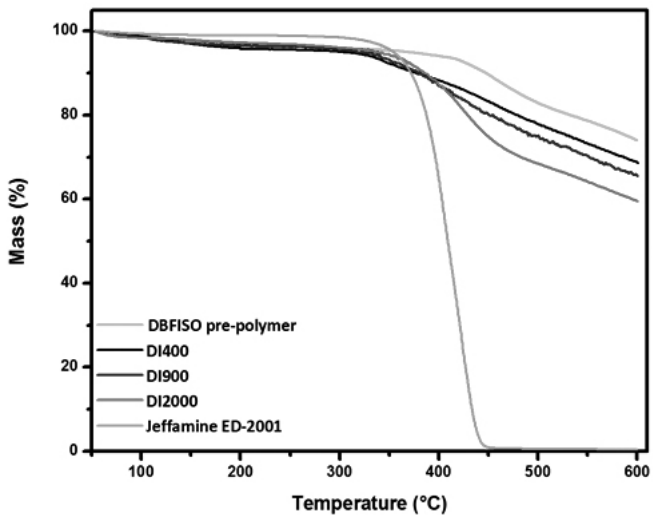

Figure 4. TGA thermograms of copoly(ether-amide)s and their component segments.

3.2. Gas transport properties of copoly(ether-amide)s

Membranes prepared from DBFISO aromatic polyamides have been reported to present low gas permeability coefficients that classifies them as gas barrier polymers[19]. Owing to the polarity introduced by the incorporation of soft polyether block segments in the polyamide backbone, the three copoly(ether-amide) membranes synthesized are more permeable than convenctional DBFISO aromatic polyamides[8,15]. Therefore, in this section, we report the gas transport properties of the block copoly(ether-amide)s and the effect of polyether block size on pure gas transport properties.

Table 2. Gas permeability coefficients and ideal permselectivities for copoly(ether-amide) membranes determined at 10 atm and 35 °C. 1 Barrer= $1x10^{-10}$ $cm^3(STP)\cdot cm\cdot cm^{-2}\cdot s^{-1}\cdot cmHg^{-1}$

Membrane	Permeability coefficient, *P* (Barrer)					Ideal selectivity, α		
	He	CO_2	O_2	CH_4	N_2	CO_2/N_2	CO_2/O_2	CO_2/CH_4
DBFISO[19]	4.22	0.32	0.07	--	--	--	4.6	--
DI400	5.17	2.83	0.35	0.15	0.09	**31.4**	**8.1**	**18.9**
DI900	4.19	1.81	0.36	0.23	0.20	9.0	5.0	7.9
DI2000	3.64	1.66	0.29	0.17	0.14	11.9	5.7	9.8

Table 2 shows the pure gas permeability coefficients, *P*, for the copoly(ether-amide) membranes evaluated at 35 °C and 10 atm. In general, all copoly(ether-amide)s show gas permeability coefficients values that are one order of magnitude higher than those presented by the DBFISO polyamide[19] with the exception of He that presents *P* values of the same order of magnitude. The DI400 copoly(ether-amide) membrane, with the shortest polyether block content and segment shows the highest CO_2 permeability coefficient and the highest ideal selectivity for the pairs CO_2/N_2, CO_2/CH_4, and CO_2/O_2. However, an increase in the polyether block size and ethylene oxide units showed a decrease in the CO_2 permeability coefficients. This behavior is attributed to the higher crystallinity found in the copoly(ether-amide)s with the larger size polyether blocks. This assumption is supported by DSC analysis (see Figure 3). These results clearly show an increase in melting temperature and enthalpy, for DSC when the polyether segment size increases[15,24]. Therefore, the presence of crystallinity in the copoly(ether-amide) membranes act as a barrier for gas permeation through the membrane. An interesting result of the incorporation of polyether segments and DBFISO aromatic polyamide blocks is the increase of CO_2 permeability coefficient and CO_2/O_2 ideal selectivity respect to the values reported for DBFISO polyamide, which increased 8.60 and 1.76 times, respectively, in the DI400 membrane. This result is attributed to the presence of polyether polar groups in the main chain. The polar groups are assumed to have dipolar interactions with the polarizable carbon dioxide molecules[22]. These interactions are stronger than the interactions between the chain segments. Thus, CO_2 breaks these interactions providing additional solubility into the polymer chain.

The diffusion coefficients (*D*) and solubility coefficients (*S*) were measured by time lag method and by the ratio of P/D respectively. Permeability and selectivity may be governed by either kinetic (*D*) or thermodynamic (*S*) parameters or both[25,26]. As shown in Table 3 the gas diffusion coefficients follow the order $D_{O_2}>D_{CO_2}>D_{N_2}>D_{CH_4}$, similar behavior has been observed for DBFISO polyamide membranes and in general for amorphous polymers[19]. The CO_2 diffusion coefficient seems to be identical in the three copoly(ether-amide) membranes and increasing slightly with increasing length of the polyether block. A different behavior was observed regarding the nonpolar gases where diffusion coefficients decreased as the content of ethylene oxide units increases, which is attributed to a higher crystalline content as molecular weight of the polyether moiety increases. On the other hand, from Table 4, it is seen that the solubility coefficients vary according to the following order $S_{CO_2}>S_{CH_4}>S_{O_2}>S_{N_2}$ which matches a behavior of increasing solubility according to the condensability of the gases. The effect of increasing the polyether segment size was more pronounced in the CO_2 solubility coefficient in which a decrease was observed as the polyether chain length increases. This decrease in solubility of this particular gas is attributed to the crystallization of the soft segment with increasing length, as shown by an increase in melting enthalpy, as determined by DSC. Moreover, crystallinity was disrupted at temperatures above 55 °C as was revealed by the decrease in the CO_2 activation energy (discussed in the temperature section). For nonpolar gases, the solubility coefficients were lower than the values found for CO_2. Overall, the increase in the CO_2 permeability coefficient and ideal selectivity are likely caused by an increases in the solubility coefficient of CO_2 in the polyether segments whose interaction is debilitated by the presence of crystalline domains in the copoly(ether-amide)s, as is revealed by higher ideal separation factors for CO_2/CH_4, CO_2/N_2, and CO_2/O_2 by solubility which were 7.5, 40.6, and 102.1 times greater respect to their diffusion selectivities. These results indicate that the solubility of the CO_2 dictates the permeation in the studied copoly(ether-amide) membranes; while for nonpolar gases, the permeation was dictated by a diffusion mechanism due to higher selectivity by diffusion, as observed in the ratio O_2/N_2.

Table 3. Gas diffusion coefficients and diffusivity selectivities for copoly(ether-amide) membranes determined at 10 atm and 35 °C.

Membrane	Diffusion coefficient, D ($\times 10^{-8}$ cm^2 s^{-1})				Selectivity by diffusion		
	CO_2	O_2	CH_4	N_2	CO_2/N_2	CO_2/O_2	CO_2/CH_4
DI400	0.75	2.64	0.47	0.85	**0.9**	**0.3**	**1.6**
DI900	0.71	1.34	0.32	0.38	1.9	0.5	2.2
DI2000	0.92	2.03	0.60	0.67	1.4	0.4	1.5

Table 4. Gas apparent solubility coefficients and solubility selectivities for copoly(ether-amide) membranes determined at 10 atm and 35 °C.

Membrane	Solubility coefficient, S ($\times 10^{-2}$ cm^3(STP)·cm^{-3}·cmHg^{-1})				Selectivity by solubility		
	CO_2	O_2	CH_4	N_2	CO_2/N_2	CO_2/O_2	CO_2/CH_4
DI400	3.77	0.13	0.32	0.10	**37.7**	**29.0**	**11.8**
DI900	2.55	0.27	0.72	0.53	11.1	9.4	3.5
DI2000	1.80	0.14	0.28	0.21	8.6	12.8	6.4

3.3. Effect of the pressure on gas permeability coefficient

Figure 5 presents gas permeability coefficients for five gases (i.e. He, CO_2, O_2, N_2, CH_4) in copoly(ether-amide) membranes at 35 ºC as a function of upstream pressure. In the three copoly(ether amide) membranes, the He permeability does not show a significant change with pressure. For the other non polar gases such as O_2, N_2, and CH_4, permeability coefficients decrease slightly with increasing pressure; this is due to fact that an increase in the hydrostatic pressure on the membrane causes a decrease in the free volume available to carry out the gas permeation. For a more condensable penetrant such as CO_2, permeability coefficient slightly increases as pressure increases. This behavior was not observed in DBFISO polyamides, and is attributed to higher CO_2 solubility and slight plasticization for the soft polyether segment presents in the copoly(ether-amide) membranes. In this case, the solubility of the gas penetrant in the membrane increases, thereby increasing the free volume; this behavior is known as plasticization phenomenon.

3.4. Effect of temperature on CO_2 permeability coefficient

The polyether segment that exist as soft block in the copolymers has been studied by DSC and details of its melting points are expected to be well understood if their correlations with CO_2 permeability coefficient could be clarified. Therefore, the temperature dependence of permeability coefficients for CO_2 through copoly(ether-amide) membranes at temperatures above and below the melting temperature of the polyether segments were studied. In general, it was expected that an increase in temperature, increases gas permeability significantly due to two factors: first, a larger mobility of the chains in the amorphous copoly(ether-amide)s phase of the membrane and second, a significant reduction of crystallinity of the polyether around 55 °C which is the melting temperature found by DSC. Figure 6 shows the relationship between the melting point of polyether segment and the CO_2 permeability coefficient, this results are similar to those reported for other copolymers containing polyether segments[14,25]; and from the figure 6, it observed a change of the slope above 55 °C. Therefore, an evaluation of the dependence of the permeability coefficients, P_{CO2}, with temperature above and below the melting point was made based in an Arrhenius type equation reported elsewhere[25]:

$$P = P_0 exp^{\left(\frac{-E_P}{RT}\right)} \qquad (4)$$

Where E_p is the activation energy for permeation, P_0 is a pre-exponential factor, R is the ideal gas constant, and T is the absolute temperature. One option to determine the difference of gas permeability coefficients above and below the melting point is by analyzing separately the activation energies for permeation, E_p, obtained from equation 4 above and below this melting point. Activation energies for permeation $E_{P_{CO_2}}$ have been summarized in Table 5. As can be seen, in all copoly(ether-amide) membranes the activation energy for permeation below 55 °C follows the order $E_{P(DI2000)} < E_{P(DI900)} < E_{P(DI400)}$, whereas above of this temperature, the $E_{P_{CO_2}}$ is almost the same value for all copoly(ether-amide)s regardless the size of the polyether block. Moreover, the activation energies for permeation are between 1.5 and 2 times higher at temperatures below 55 ºC, which is attributed to the presence of crystallinity in the copoly(ether-amide)s. These results will imply that CO_2 interaction with the polar segments is similar in the amorphous phase. Thus, at temperatures above the melting point of the crystalline phase the activation energy for CO_2 permeation remains constant.

Table 5. Activation energies for permeation of CO_2 below and above melting point of the polyether segment in copoly(ether-amide) membranes.

Membrane	Activation energy for permeation, E_P (kJ/mol)	
	35-55 °C	55-75 °C
	CO_2	CO_2
DI400	24.76	14.40
DI900	29.91	19.64
DI2000	38.49	14.91

For all the copoly(ether amide) membranes tested E_p lowers at temperatures above the melting point are an indication that the crystalline phase was reduced facilitating the permeability of the gases thorough the membrane. These results are consistent with previously reported $E_{P_{CO_2}}$ in other copolymers containing polyether. Kim et al.,[14] reported values below and above (50 °C) the melting point of PEBAX® 1657 aliphatic copoly(ether-amide) of 14.6 and 10.9 kJ/mol, respectively. Also, Tocci et al.,[27] carried out determinations of $E_{P_{CO_2}}$ in a temperature range of 25 to 85 °C, they reported activation energies for CO_2 permeation below 60 °C (18.19 kJ/mol) and above 60 °C (8.41 kJ/mol), which show the same behavior found for aromatic copoly(ether-amide)s in this work.

4. CONCLUSIONS

The gas transport properties of DBFISO aromatic polyamide, which is considered a gas barrier polymer, were modified by the incorporation of soft polyether segments of different molecular weight. The results of pure gas permeability for the copoly(ether-amide) membranes revealed that CO_2 was more permeable than other gases, which is attributed to a high affinity between CO_2 and the ether bonds of the polyether segments. In addition, an increase in polyether segment size (molecular weight) does not enhance the gas permeability of the copoly(ether-amide) membranes since the best performance for CO_2 permeability and selectivity was obtained in the DI400 membrane which has the smallest polyether segment. In this membrane, CO_2 permeability coefficient was 8.6 times larger than the one reported in DBFISO aromatic polyamide. It was also found that gas transport properties were not improved as polyether segment size increases; this behavior was due to polyether crystallization as revealed by DSC studies. In addition, it was found that the activation energy for CO_2 permeation is considerably larger when the polyether segment crystallizes. The results obtained indicate that in order to

increase permeability and selectivity for CO_2 systematic studies in which an increase in polyether concentration, with the shortest segment to diminish the possibility of crystalline phase formation, could increase permeability and selectivity of copoly(ether-amide) membranes.

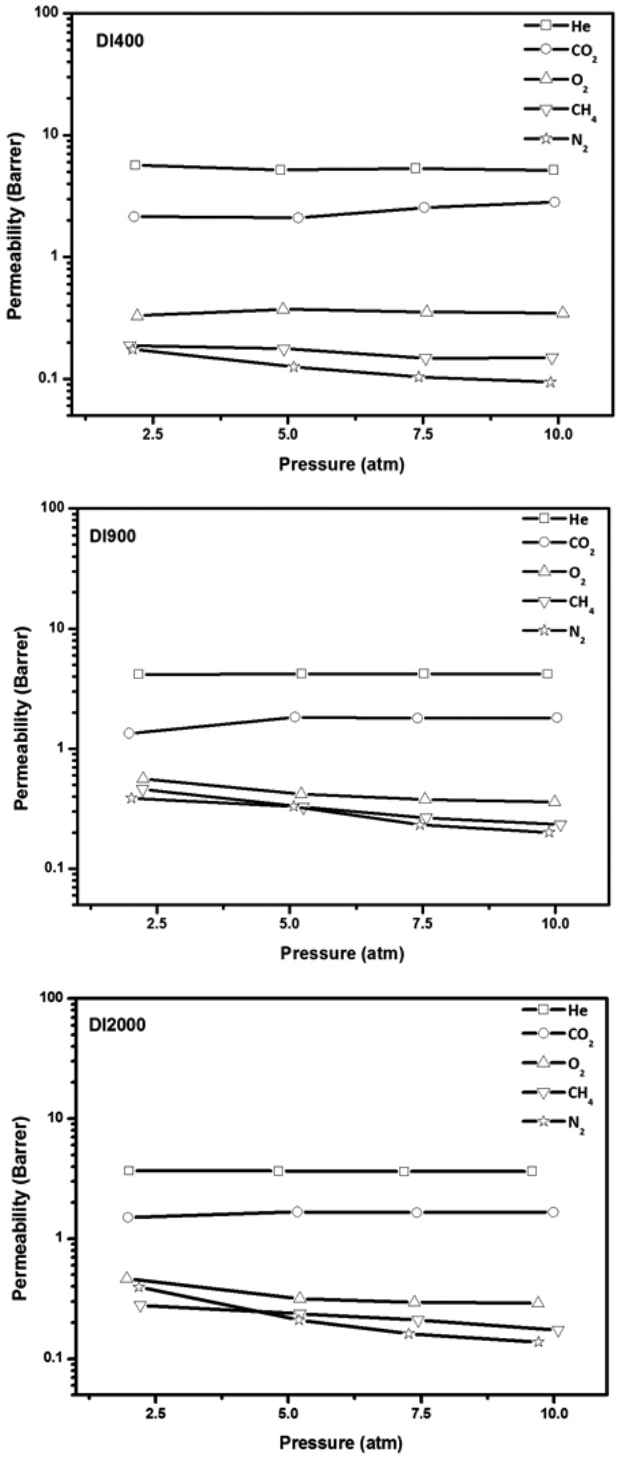

Figure 5. Effect of pressure on permeability coefficients in copoly(ether-amide) membranes evaluated in the pressure range of 2.0 to 10.0 atm at 35 °C.

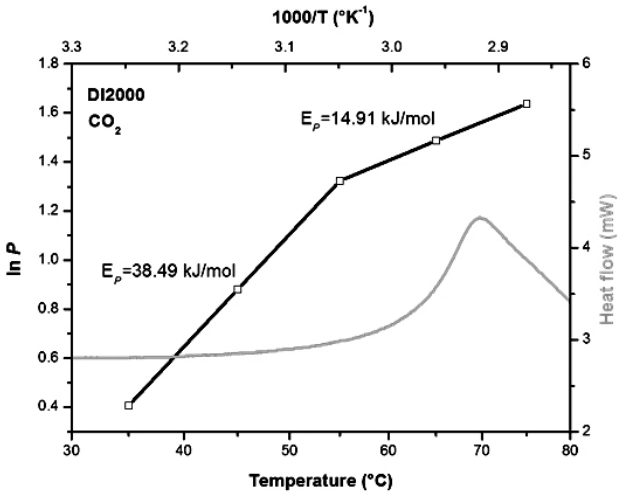

Figure 6. Illustration of the activation energy change for CO_2 permeation determined below and above melting temperature of the polyether component present in the copoly(ether-amide) membranes.

ACKNOWLEDGEMENTS

The research reported was performed under grant CONACyT-México No. 41437. The authors would like to acknowledge the partial support from FOMIX-Yucatán project No.108920. Julio Sánchez thanks FONDECYT (grant No. 11140324) and CIPA, Chile.

REFERENCES

1. D.F. Sanders, Z.P. Smith, R. Guo, L.M. Robeson, J.E. McGrath, D.R. Paul, B.D. Freeman, *Polymer* **54**, 4729, (2013)
2. Y. Zhang, J. Sunarso, S. Liu, R. Wang, *Int. J. Greenh. Gas Con.* **12**, 84, (2013)
3. Z. Y. Yeo, T.L. Chew, P.W. Zhu, A.R. Mohamed, S-P. Chai, *J. Nat. Gas Chem*. **21**, 282, (2012)
4. B.D. Freeman, *Macromolecules* **32**, 375, (1999)
5. A.L. Kohl and R.B. Nielsen, *Gas purification*, 5th Ed. Gulf Publishing Company, Houston Texas, USA, 1997.
6. A. Kargon and M.T. Ravanchi, in *Greenhouse gases: capturing, utilization and reduction*, G. Liu ed., InTech, 2012; chapter 1.
7. B. Shimekit and H. Mukhtar, in *Advances in Natural Gas Technologies*, Ed. H.A. Al-Megren, InTech 2012; Chapter 9.
8. H. Lin and B.D. Freeman, *J. Mol. Struct.* **739**, 57, (2005)
9. H. Lin, E.V. Wagner, B.D. Freeman, L.G. Toy, R.P. Gupta, *Science* **311**, 639, (2006)
10. J.E. Bara, C.J. Gabriel, E.S. Hatakeyama, T.K. Carlisle, S. Lessmann, R.D. Noble, D.L. Gin, *J. Membr. Sci*. **321**, 3, (2008)
11. V.A. Kusuma, B.D. Freeman, M.A. Borns, D.S. Kalika, *J. Membr. Sci*. **327**, 195, (2009)
12. H.W. Kim and H.B. Park, *J. Membr. Sci*. **372**, 116, (2011)
13. S.L. Liu, L. Shao, M.L. Chua, C.H. Lau, H. Wang, S. Quan, *Prog. Polym. Sci*. **38**, 1089, (2013)
14. J. H. Kim, S.Y. Ha, Y.M. Lee, *J. Membr. Sci*. **190**, 179, (2001)
15. H. Lin and B.D. Freeman, *J. Membr. Sci*. **239**, 105, (2004)
16. E.M. Maya, D.M. Muñoz, J.G. de la Campa, J. de Abajo, A.E. Lozano, *Desalination* **1999**, 188, (2006)
17. A. Car, C. Stropnik, W. Yave, K.V.J Peinneman, *J. Membr. Sci*. **307**, 88, (2008)
18. H. Husken, T. Visser, M. Wessling, R.J. Gaymans, *J. Membr. Sci.* **346**, 194, (2010)
19. C. Carrera-Figueiras, M. Aguilar-Vega, *J. Polym. Sci. Part B: Polym. Phys.* **45**, 2083, (2007)
20. N. Yamazaki, M. Matsumoto, F. Higashi, *J. Polym. Sci. Polym. Chem. Ed.* **13**, 1373, (1975)
21. M.I. Loría-Bastarrachea, M. Aguilar-Vega, *J. Appl. Polym. Sci.* **103**, 2207, (2007)
22. S.R. Reijerkerk, A. Arun, R.J. Gaymans, K. Nijmeijer, M. Wessling, *J. Membr. Sci.* **359**, 54, (2010)

23. M.J. van der Schuur, R.J. Gaymans, *Polymer* **48**, 1998, (2007)
24. D.M. Muñoz, E.M. Maya, J. de Abajo, J.G. de la Campa, A.E. Lozano, *J. Membr. Sci.* **323**, 53, (2008)
25. W.J. Koros, M.R. Coleman, D.R.B. Walker, *Annu. Rev. Mater. Sci.* **22**, 47, (1992)
26. S. Matteucci, Y. Yampolskii, B.D. Freeman, I. Pinnau, In *Materials Science of Membranes for Gas and Vapors Separation*, Yampolskii Y.; Pinnau I.; Freeman B.D. Eds., Jhon Wiley & Sons, Chichester, England, **2006**, pp. 1-47.
27. E. Tocci, A. Gugliuzza, L. de Lorenzo, M. Macchione, G. de Luca, Drioli E, *J. Membr. Sci.* **323**, 316, (2008)